Formation and optical properties of laser-active N_2 centers in KCl

Efstratios Georgiou
Department of Physics and Materials Science Center, Cornell University, Ithaca, New York 14853

Clifford R. Pollock
School of Electrical Engineering and Materials Science Center, Cornell University, Ithaca, New York 14853

(Received 21 January 1991; revised manuscript received 15 July 1991)

Recent experimental results on the formation and optical properties of the laser-active N_2 center in additively colored pure KCl are reported. The N_2 center in KCl is most efficiently formed through a photoaggregation process in heavily colored crystals exposed to light on the long-wavelength shoulder of the F band. The observed room-temperature stability of the N_2 center indicates that it is an electrically neutral defect. Absorption and emission bands peak at 1.02 and 1.25 μm, respectively. The N_2-band absorbance grows proportionally with the R_1- and R_2-band absorbances. Polarized N_2-center fluorescence data is consistent with two degenerate orthogonal dipole moments lying on {111} planes of the crystal. Excited-state absorption spectra show higher transitions coincident in wavelength with the R_1 and R_2 absorption bands of the trigonal F_3 color center in KCl. Similar experiments on the R_1 band correlate well with the N_2-center data. Results are consistent with the identification of the laser-active part of the N_2 band as a transition of the trigonal F_3 color center.

I. INTRODUCTION

Color-center aggregates consisting of three or more F centers have been studied for almost 40 years in various alkali halide hosts.[1-10] Several absorption bands due to these aggregate centers are observed in the visible and near-ir spectral regions. The best known are the so-called R and N bands, although, in the case of the N bands, the identification of the exact structure of the corresponding centers is still a subject of controversy.[4-9]

It is generally recognized that both the R_1 and R_2 bands, lying between the F and F_2 primary absorption bands, are due to transitions of the "trigonal F_3" color center (Fig. 1), which consists of three adjacent F centers in an equilateral triangle configuration.[4,6,7,11] However, the nature of the N_1 and N_2 absorption bands, which lie at longer wavelengths than the F_2 band, is not established. Several models have been proposed for these bands, based on various F_3 and F_4 aggregate configurations.[4,5,7,8] Experimental data and interpretations regarding the nature of the N transitions sometimes appear contradictory. For example, the N_1 band in NaCl is believed by some researchers to arise from a planar F_4 configuration.[4,9] Other experiments in KCl have supported an F_4 structure for the N_2 band but not for the N_1 band.[5] More recent work, however, suggests that both the N bands in KCl—as well as the shorter-wavelength R_1 and R_2 bands—arise from the trigonal F_3 color center.[7,8] Other possibilities have not yet been unambiguously disproven by experiment. Evidence of several overlapping absorptions in the N-band region,[8,12,13] and the absence of zero-phonon lines associated with the main N_1 and N_2 bands in pure KCl,[8,14,15] make the identification of the N-center structure very difficult.

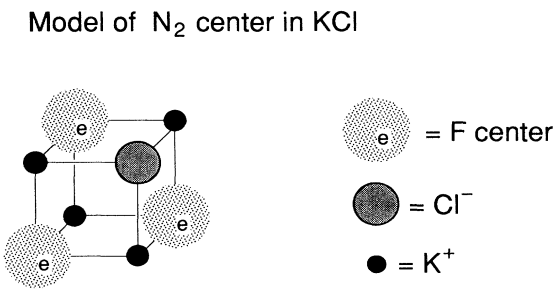

FIG. 1. Proposed configuration of the N_2 center in KCl (in the text we refer to this as the "trigonal F_3" model).

Recently we demonstrated that the N_2 center in KCl is a laser-active defect.[16] Several features of the KCl N_2-center system, such as the simple formation process, tunability in the 1.23–1.35-μm range, and infinite operational lifetime, make it a useful laser medium. There is a strong possibility that this laser can also be created in other host lattices. Further interest arises from the fact that this is the first multi-electron color-center laser demonstrating long-term operational stability. In this paper we provide experimental evidence that the particular lasing N_2 center is a trigonal F_3 defect (as shown schematically in Fig. 1). Excited-state spectroscopy data strongly correlates the N_2 transition with the R_1 and R_2 transitions of the trigonal F_3 center. The optimum formation procedure has also been examined, as well as optical properties of the center that are relevant to laser operation.

II. EXPERIMENTAL METHODS

Visible and near-infrared absorption spectra were taken in a custom dual-beam spectrometer described else-

where.[17] The same apparatus was also used for the fluorescence and excited-state spectroscopy experiments. The crystal was mounted on the cold finger of an optical vacuum dewar capable of maintaining temperatures from 77 to 360 K. The crystal was oriented so that a ⟨001⟩ direction was lying along the spectrometer optical axis. A variety of light sources were used for color-center photoaggregation. Light in the 350–600-nm spectral range was provided by a filtered 100-W mercury arc lamp. A combination of GG-495 and KG-3 Schott filters was employed to selectively transmit the green Hg spectral lines (546 and 579 nm), while KG-3 and 4-97 Corning filters were used to transmit blue and green spectral lines (365, 405, 436, 546, and 579 nm). Red light illumination was obtained from either an incandescent source filtered through a band-pass interference filter (620–660 nm), or from an expanded 5-mW He-Ne laser beam(633 nm).

For pumping the centers to excited states, laser radiation was injected as close as practically possible to the [001] direction of the crystal ($\approx 1°$ off-axis). For the polarized emission experiments the pump laser beam was incident precisely along the [001] crystal axis.

All spectral data has been taken at 77 K, unless otherwise specified.

III. FORMATION OF N_2 COLOR CENTERS

Single KCl crystals were grown using the Kyropoulos technique at the Crystal Growth Facility at Cornell University. To ensure that the color centers under study are not associated with any impurity, boules grown from different stocks of nominally pure KCl material were tried. Additionally, UV spectra were taken to verify the absence of oxygen impurities. Although no impurity in the host crystal is necessary for the laser-active center formation, common impurities typically found in alkali halides, such as other alkali-metal ions or OH^-, do not prevent the formation of the N_2 centers;[14,18] for example, the process that is described below produced N_2 centers in KCl crystals doped with either Li^+ or OH^-.

Crystals cleaved to 3-mm thicknesses were additively colored in potassium vapor at 600 °C, either in a heat-pipe or in a stainless-steel bomb, and then rapidly quenched to room temperature. Bomb coloration was preferred over heat-pipe coloration whenever higher vapor pressure (≈ 140 Torr) was desired. Fast quenching was important in order to prevent formation of F-center colloidal aggregates, which reduce the crystal optical transmission over extended spectral regions. Colored crystals were handled and polished under regular room light, although care was taken to minimize the total exposure.

The absorption spectrum of a KCl crystal that has been additively colored [Fig. 2(a)] shows bands due to F centers (peak at 542 nm), F_2 centers (peak at 803 nm), and R ($=F_3$) centers (peaks at 656 and 730 nm), as well as trace N_1- and N_2-band absorptions (peaks at 968 and 1019 nm). In fast quenched samples the initial R- and N-band absorbances were negligible. Formation of significant N_2-center populations in the colored KCl crystals can be accomplished with a photoaggregation process using F-band light. This process is thought to ionize F centers, producing anion vacancies (α centers) which are thermally mobile at temperatures above ≈ 240 K.[19] These subsequently combine with other centers to create higher aggregates, among them N centers [Fig. 2(b)]. The peak absorbances of the most important color center bands in KCl are plotted in Fig. 3 as functions of photoaggregation time. These graphs are in agreement with data from previous work.[20] The F band gradually

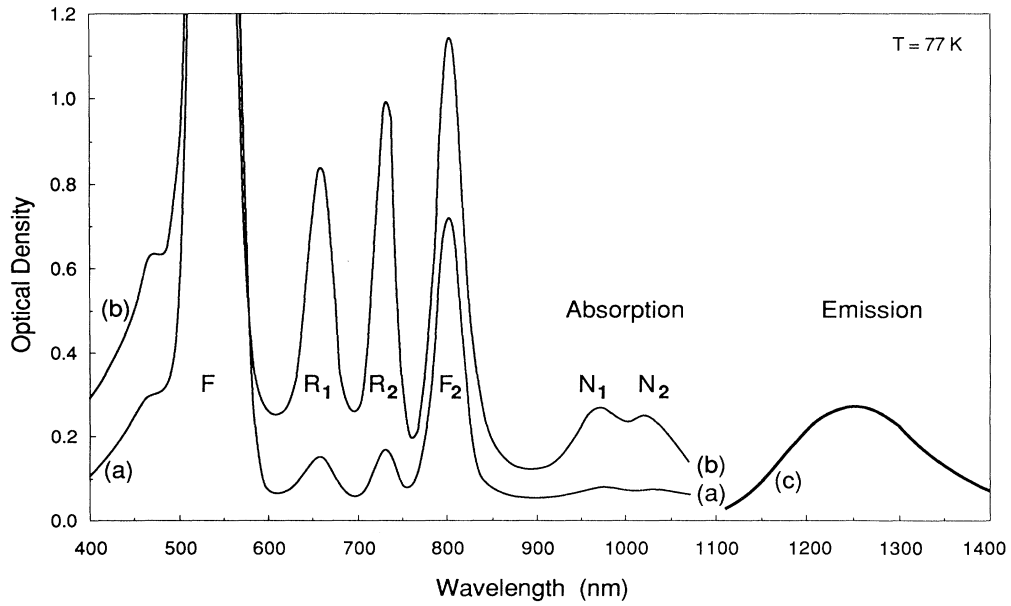

FIG. 2. (a) Absorption spectrum of pure KCl slab following additive coloration. (b) Same, following photoaggregation. (c) N_2-band emission spectrum. A 1.06-μm Nd:YAG laser was used for the N_2 center excitation.

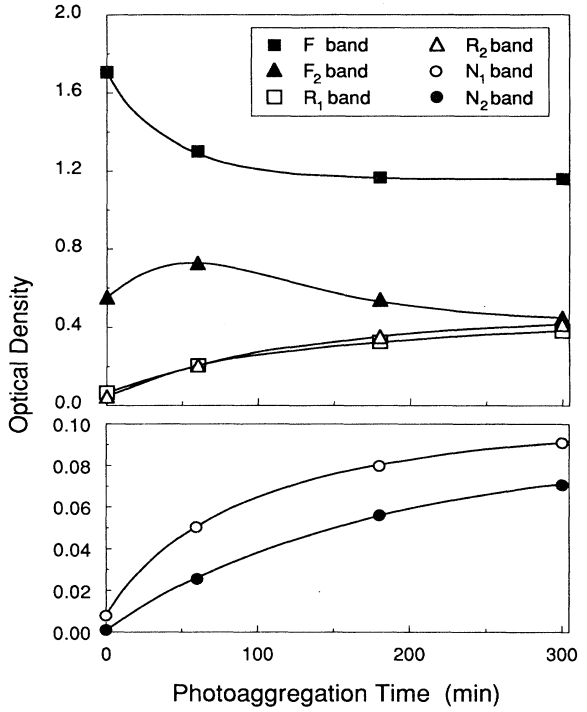

FIG. 3. Optical densities of various color-center bands in KCl as a function of photoaggregation time.

bleaches, the F_2 absorption initially increases and subsequently decreases, while the R (i.e., F_3) and N bands show a continuous increase that approaches saturation. In our crystal-sample preparation we continued the photoaggregation until this approximate steady state in the band formation was reached. This required several hours, depending on the temperature, crystal thickness, and light source used. Prolonged photoaggregation beyond this point eventually led to slow formation of colloidal color-center aggregates, characterized by reduced crystal transmission in broad regions of the visible and near-ir optical spectrum.

Upon completion of the photoaggregation process, the final N_2 absorbance was found to be an increasing function of the initial coloration vapor pressure.[21] A purer N_2 population resulted from higher coloration pressures (>100 Torr), as was evident from absorption and excited-state measurements. In lightly colored crystals (colored at 20-Torr vapor pressure or lower) a shoulder absorption was observed on the long-wavelength side of the N_2 band. It was also found that in heavily colored crystals the N_2 peak was more clearly resolved from the adjacent N_1 band, and the N_2- to N_1-absorbance ratio was higher. Significant differences between lightly and heavily colored crystals were also observed in the N_2 excited-state absorption spectra, as will be described later, indicating the presence of a variety of centers with overlapping absorptions. In general, it appeared that the N_2 band was more homogeneous in the densely colored crystals. Furthermore, we could always obtain N_2-center laser action in heavily colored crystals, while this was not always the case in lightly colored ones. Therefore, we preferred to use heavily colored crystals in all the experiments in which it was practical.

N_2-center formation was found to be most efficient when photoaggregation was performed at temperatures around 260 K. Temperatures much below 260 K simply slowed the aggregation process, requiring impractically long photoaggregation times (>15 h). Room-temperature photoaggregation led to the formation of a long-wavelength shoulder absorption, overlapping the N_2 absorption band and extending into the spectral region of the N_2-center emission.[21]

Variations in the spectral distribution of the light used for photoaggregation affect both the N-center formation rate and the resulting N_2/N_1 absorbance ratio. Best results, as far as the N_2 band is concerned, were achieved using red light (i.e., light on the long-wavelength side of the KCl F band), usually obtained from a 5-mW 633-nm He-Ne laser beam (expanded for uniform crystal illumination). Use of this light resulted in the highest N_2- to N_1-absorbance ratio (Fig. 4) and the clearest separation between the N_2 and N_1 band peaks. Another advantage of using red light was that it was not severely attenuated in the crystal by the extremely dense F-band absorption, therefore uniform aggregation could be achieved. Use of green Hg-lamp lines or the 515-nm Ar^+-laser line for crystal illumination yielded similar aggregation rates to those obtained with the He-Ne light, but was slightly less efficient in N_2-center formation. Finally, use of all blue and green Hg-lamp lines (365 to 579 nm) for photoaggregation dramatically enhanced the N_2-formation rate,[21] but led to a much lower N_2- to N_1-absorbance ratio (Fig. 4), and resulted in N_2-laser crystals with reduced performance. Also, in this case, the N_2 band was poorly resolved from the N_1, and the N_2 peak

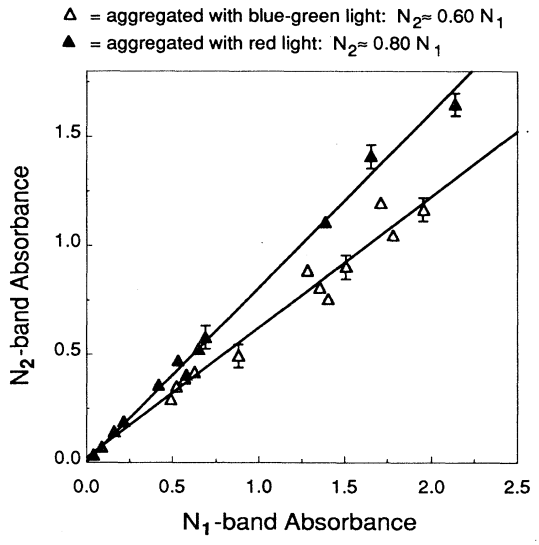

FIG. 4. Effect of spectral distribution of aggregating light on the formation of the N_2 vs the N_1 band in KCl.

was indistinct. It appears that short-wavelength light causes the formation of other centers having absorptions that overlap the two N bands. These spurious centers were more evident in thin samples, probably due to absorption of the shorter wavelengths near the crystal surface.

Slow aggregation effects, characterized by R and N center formation and simultaneous F_2-band bleaching, were also observed under crystal illumination at 260 K with broadband light in the 750- to 1000-nm wavelength region.[22] Here our observations agree with those reported in Ref. 11 and quoted in Ref. 6, but disagree with the findings of Refs. 23 and 24. The observed transformations indicate that, when optically excited in their fundamental absorption, the F_2 centers randomly walk in the lattice, combining with the abundant F centers to form F_3 aggregates (or, less probably, with other F_2 centers to form F_4 aggregates). In contrast, no aggregation effects were observed under the action of 1 W of 1.06-μm Nd:YAG laser light, even after several hours of illumination of 260–300 K. This indicates that the N_2 centers do not become mobile in the lattice under optical excitation of their fundamental absorption.

The collective absorption data, compiled from more than 30 different crystal samples at various stages of the photoaggregation process, show a linearity between the R_1 and the N_2 band absorbances (Fig. 5). The correlations between the R_1 and R_2 and between the R_1 and N_1 bands are also shown for comparison. Fluctuations from the linear behavior are attributed to uncertainty in estimating the background absorbance (this background was subtracted from all absorbance values), and also to the potential presence of other absorptions overlapping the main R and N bands. These effects are more serious in the case of the N-band absorptions, which are weaker and broader relative to the R bands. In spite of rather minor deviations, the linearity between the R- and N-band absorbances over a wide range of values, evident from Fig. 5, indicates that all these bands are due to aggregate defects consisting of equal numbers of F centers. This conclusion agrees with the majority of similar studies on the growth of the KCl R_1, R_2, and N_2 bands during photoaggregation.[7,20,25] In previous literature the growth of the N_1 band is generally found inconsistent with that of the other R and N bands, indicating the presence of several absorptions under the N_1 band.[12,20,25] Several experimental observations presented in this work (for example, Fig. 4 data) agree with this point, although the Fig. 5 collective data averages out inconsistent growth trends and does not reveal any systematic nonlinearity in the N_1 band growth relative to the others.

Following photoaggregation, the crystals can be stored at room temperature in the dark without any apparent degradation in the N_2 absorption band for time periods of at least a few weeks. Laser crystals that were stored at room temperature in the dark for over a week and then reused in the laser without any reprocessing, yielded the same output power as in their initial use.[16] In pure KCl this room-temperature thermal stability suggests that the N_2 laser-active center is a neutral defect.[12]

The N_2 band is known to bleach thermally at elevated

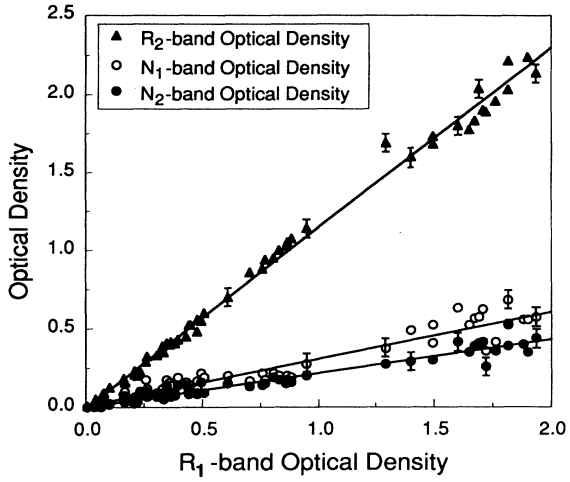

FIG. 5. R_2, N_1, and N_2 vs R_1 absorbance correlation diagrams. Data points correspond to crystals processed with aggregating light of any spectral distribution, as described in the text.

temperatures, accompanied by a corresponding decrease in the R bands and an increase in the N_1 absorption.[8,13,20,25] Upon heating of the colored crystals to 360 K for 100 min we observed similar spectral changes as those reported in the quoted references. These changes had been interpreted in the past as evidence that the N_1 and N_2 bands arise from different centers.[20] While this may indeed be true, we observed that the thermally-produced N_1 band in our samples is shifted by about 10 nm to the bue relative to the initial (optically produced) N_1 band. This indicates that there exist at least two distinct types of N_1 centers. Schneider[8] has shown with fluorescence experiments that there exist four different bands under the N_1 absorption, all having different emission properties, and has proposed various models for the corresponding color centers. The wavelength coincidence of so many narrow absorption bands, which belong to dissimilar centers, is remarkable and rather unexpected.

IV. ABSORPTION AND EMISSION PROPERTIES

The N_2 absorption band in KCl [Fig. 2(b)] at 77 K peaks at 1019 nm with a 54 nm ($\approx$0.063 eV) full width at half maximum (FWHM). At higher temperatures this band shifts to longer wavelengths and broadens. Typically, N_2-band peak optical densities of approximately 4 O.D./cm were achieved in heavily colored KCl laser crystals following photoaggregation, indicating density of approximately 1.7×10^{16} N_2 centers/cm^3. The N_2 band conveniently overlaps the 1064-nm line of the Nd:YAG laser, which was used for all fluorescence and laser studies. Using this laser line for the optical excitation of the N_2 centers has the added advantage of avoiding excitation of the adjacent N_1 band, thus improving the reliability of the obtained data relative to previous similar experimental works that have used broadband light.[7,8,26,27]

The N_2 emission band peaking at 1.25 μm [Fig. 2(c)] is slightly asymmetric and much broader (FWHM $=174$ nm, or ≈ 0.138 eV) than the absorption band. Practically identical emission curves are obtained by pumping the colored KCl crystal at several other visible and near-ir wavelength regions.[7,8,11,28] The full excitation spectrum for the 1.25-μm emission has been shown to have peaks coinciding with the F, R_1, R_2, M $(=F_2)$, N_1, and N_2 bands.[7,11] This argument has been the basis of the hypothesis that both N absorptions represent transitions of the F_3 center from the ground to the lowest excited states, while the other peaks (F,R,M) correspond to higher transitions of the same center. Silsbee[7] gave theoretical support to this model, along with interpretation of several experimental results. Since we noticed differences in the N-band formation using different photoaggregation methods, we experimentally recompared the N_2-band emission with the emission obtained from some other color-center bands. We verified that the R_1 band, pumped with a 633-nm He-Ne laser, yields a fluorescence curve identical to that obtained from N_2 centers, and that the N_1 band, pumped with a 940-nm LED, also yields fluorescence peaking at 1.25 μm (in the latter case the resolution of the emission peak was poorer, due to the lack of an intense monochromatic pump source).

The radiative lifetime of the N_2-center emission at 77 K has been measured to be 205 nsec (± 10 nsec), using pulsed (20 nsec) Nd:YAG laser pumping. This lifetime starts decreasing rapidly above 150 K (Fig. 6), suggesting the onset of phonon-assisted nonradiative decay processes from the first excited state. Despite that, as the crystal temperature is raised from 77 K, the measured emission intensity at 1.25 μm initially increases. This is due to the red-shifting and broadening of the absorption band, which cause increased overlap with the 1.064-μm pump wavelength. If the absorbed power at 1.064 nm is taken into account, the resulting normalized emission intensity shows a monotonic decrease versus temperature (Fig. 6), indicating a corresponding decrease of the pump-cycle quantum efficiency.

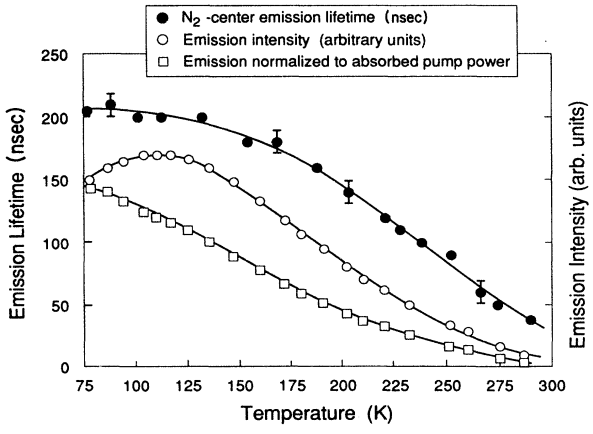

FIG. 6. N_2-center emission lifetime in KCl as a function of temperature. Fluorescence signal intensity is also plotted for comparison.

V. EXCITED-STATE SPECTROSCOPY OF N_2 CENTERS

To characterize the structure and electronic nature of a color center, a useful tool is the experimental mapping of the excited-state transitions of the defect and comparison of this data with the predictions of particular theoretical models.

N_2-center excited-state transitions were probed using a technique developed by Chiarotti and Grassano.[29] The experimental setup has been described in detail in our previous work;[17] minor differences will be noted below. This technique is based on modulating the populations in the ground and first-excited states of a defect, and then monitoring the modulation of the absorption transitions which originate from each of these two levels. Population modulation is achieved with a chopped pump laser that excites the transition from the ground to some excited state. Other absorption transitions originating from these two states are revealed from the resulting modulation in the absorption spectrum of the sample. Transitions from the first excited state to higher energy levels can only occur when the pump is on, resulting in reduced transmission at the corresponding wavelengths (modulation signal out-of-phase with the pump). At the same time, when the pump is on, there are fewer transitions from the ground state to excited states, resulting in increased transmission at the corresponding wavelengths (modulation signal in-phase with the pump). The detection of these small transmission changes is achieved with a lock-in amplifier referenced to the chopping frequency of pump beam. The chopping period has to be sufficiently longer than the emission lifetime of the defect, so that the population modulation can follow the pump cycles. At the same time, it is also desirable that the chopping period be short, so that changes occurring over longer time scales, such as crystal heating or long-lived transitions of other interfering centers, are not simultaneously detected. Heating effects can cause significant modulation of the transmission at the color-center band peaks,[21] since it is known that upon temperature rise the color-center bands broaden. However, this problem can be avoided by using chopping speeds on the order of a few kHz.

A cw Nd:YAG laser modulated at 50% duty cycle was used to excite the fundamental transition of the N_2 center. The modulation frequency could be varied continuously between 0 and 15 kHz; however, the signal to noise ratio (SNR) degraded significantly above 2.5 kHz. Several scans were taken, which showed that the obtained excited-state spectrum was practically independent of the frequency for frequencies above 1 kHz; therefore, we subsequently used a 2-kHz chopping frequency as the most reliable compromise. Since several properties of the N_2 center are strongly temperature dependent, the total pump power absorbed in the crystal was kept below 300 mW in order to avoid heating effects. At higher power levels a better SNR could be obtained; however, the resulting spectra were altered. The pump beam was weakly

focused on a 1-mm^2 area of the sample. The monochromater slit was partially masked, so that only light from the sample area being pumped was admitted.

We noticed significant differences in the excited-state spectra depending on the previous photoaggregation procedure and the pressure at which crystals had been colored. Since our best laser results were obtained with heavily-colored crystals aggregated with red light, we used a similar bomb-colored sample for the experiments described here. To avoid excess light absorption and SNR degradation, a very thin (0.2 mm) crystal sample was used, cleaved from the center of a thicker piece. This sample had sufficient transmission ($>5\%$) to provide a useful signal over most of the spectral region of interest, except around the F-band peak (from 505 to 565 nm). In this region it was necessary to "patch" the excited-state spectrum with data obtained from other crystals colored at lower pressures. The excited-state signal was finally normalized to the crystal transmission value at each wavelength, in order to obtain the correct relative strengths of the excited-state bands.

The excited-state spectrum obtained for the N_2 system in KCl is shown in Fig. 7. Positive and negative signals in this graph correspond to transitions originating from the ground state and from the first excited state, respectively. The most obvious features of the graph are the prominent positive peaks at 657 and 731 nm, coinciding with the peak wavelengths of the R_1 and R_2 KCl bands. This result strongly supports the trigonal F_3 model for the N_2 center, since, on the basis of this model, the N_2, R_1, and R_2 transitions all originate from the ground state of the F_3 defect (Fig. 8 and Refs. 7, 30, and 31).

The observed excited-sate spectrum also shows three other weaker transitions. One of these (537 nm) lies in the F-band region and corresponds to excitation from the ground state to the R_F level shown in Fig. 8. Another positive transition signal in the F_2-band region (813 nm)—superimposed on a broad competing negative signal extending between 750 and 950 nm—corresponds to excitation from the ground state to the R_M level in Fig. 8.

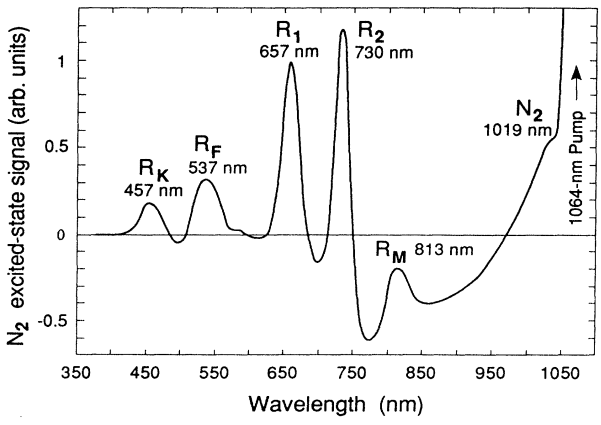

FIG. 7. Excited-state spectrum of N_2 centers in KCl, pumped with a 1.06-μm cw Nd:YAG laser.

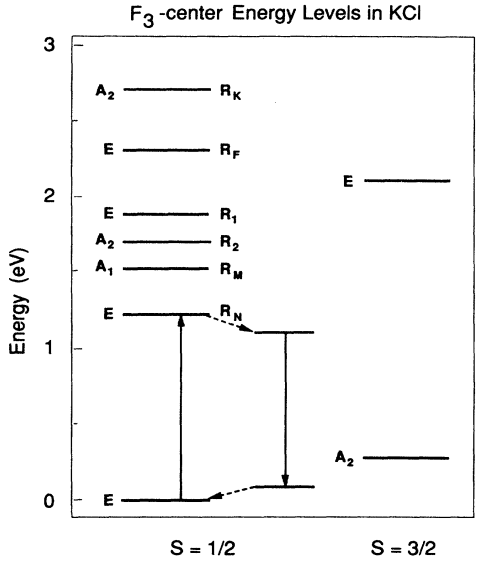

FIG. 8. Energy levels of the trigonal F_3 center in KCl (figure adapted from Ref. 7). The arrows designate the N_2 transition (absorption in normal center configuration and emission in relaxed configuration). Energy levels are as determined by experiment. $S=\frac{3}{2}$ levels are quoted from Refs. 30 and 31.

Since both the F- and F_2-region transitions are predicted by the F_3 model,[7] their presence in the excited-state spectrum of the N_2 center constitutes further evidence for the validity of this model. The transition at 457 nm coincides with the R_K level, reported in Ref. 7; however, a broad R_B transition (peaking at 620 nm) quoted in the same work was not observed here. The absence of the R_B transition in our spectra is not particularly disturbing, as the existence of this state has never been unambiguously established, and, furthermore, some theoretical calculations do not predict it either.[32]

The broad negative band extending between 700 and 950 nm is difficult to interpret, since no calculation on F_3 transitions between higher excited states is available. This feature can either correspond to several closely spaced transitions from the first-excited N_2 level to higher states, or it might be spurious interference from other N centers that are simultaneously excited.

The results of the excited-state experiments on the N_2 center in KCl are summarized in Table I, along with theoretical calculations of F_3-center transition energies.[33–35] Only the observed transitions that can be unambiguously attributed to the N_2 center are listed. The labeling of the bands and the notation of the transitions follow the trigonal F_3-model interpretation of the data. The agreement between experiment and theory is fair. Silsbee's values for the R-center transition energies, obtained from stress-induced dichroism experiments,[7] are also listed for comparison. The agreement between our N_2-center data and Silsbee's R-center data is excellent, and it can be considered as one of the strongest arguments in favor of the trigonal F_3 model for the N_2 center.

TABLE I. Observed and calculated transition energies (in eV) of the N_2 center in KCl, in the trigonal F_3 model interpretation. Transitions are between states with spin $S=\frac{1}{2}$. Asterisks indicate that data is unavailable.

Band	Transition	Observed ΔE in this work	Observed ΔE by Silsbee (Ref. 7)	Calculated ΔE (Ref. 33)	Calculated ΔE (Ref. 35)	Calculated ΔE (Ref. 34)
R_K	$^2E^e \rightarrow (^2A^e)_2$	2.71	2.67	2.81	2.57	2.75
R_F	$^2E^e \rightarrow {}^2E^0$	2.31	2.44[a]	*	2.62	2.72
R_1	$^2E^e \rightarrow {}^2E^e$	1.89	1.89	1.96	2.06	1.60
R_2	$^2E^e \rightarrow (^2A^e)_2$	1.70	1.70	1.93	1.47	1.72
R_M	$^2E^e \rightarrow (^2A^e)_1$	1.53	1.52	*	2.15 or 0.43[b]	1.16
R_N	$^2E^e \rightarrow {}^2E^e$	1.22	1.22	*	1.28	1.18

[a]Value quoted from Ref. 27.
[b]No satisfactory calculated value for this transition.

It was not possible to verify whether the relative R_1, R_2, and N_2 oscillator strengths, as obtained from the excited-state spectrum data, are equal to the strengths obtained from the absorption spectrum data, because of the poor pump-light rejection in the region of the N_2 band. Another source of difficulty is the presence of the broad negative band (750-950 nm) in the excited-state spectrum. A reliable comparison would give more evidence about the presence of other centers with absorption bands overlapping the N_2 band.

A rather surprising feature of the N_2-center excited-state spectrum is the consistent lack of a peak corresponding to the N_1 band. In principle, this suggests that the N_1 center is of a different nature, despite the previous interpretation of the N_1 band as an energy level of the trigonal F_3 center in both theoretical and experimental discussions.[7,8] However, the possibility of cancellation of an N_1 transition in the excited-state spectrum by an overlapping competing transition cannot be totally excluded. For example, such a competition could result either from an allowed 1.28-eV transition from the first excited N_2 state to some higher level, or from the creation of other short-lived centers through an electron-transfer process. Nevertheless, as will be further argued in the discussion section, we consider such coincidental cancellations rather unlikely.

To cross-check the results of the excited-state spectra that correlate the R_1, R_2, and N_2 bands, we performed similar experiments on the excited states of the R_1 center. To pump the R_1 transition we used a 5-mW 633-nm He-Ne laser, in the same setup used for the N_2 excited-state experiments. The low power of the He-Ne pump resulted in poor SNR and data from 16 scans were averaged to obtain the graph of Fig. 9. Data was still not considered reliable in the 400–600 nm region due to noise problems, and the same applies to the region around the 633-nm pump wavelength, due to poor rejection of the pump light. An additional problem was the presence of strong R-center fluorescence which distorted the measurement in the 900-nm and longer wavelength region. In this region the estimated fluorescence signal was subtracted from the actual excited-state data; however, the process might be prone to systematic errors. Compared with the case of the N_2 center, the R_1 excited-state spectrum shows peaks corresponding to the same transitions from the ground state to higher states, i.e., the R_K, R_F, R_1, R_2, R_M, and N_2 transitions; here, also, no transition is observed at the N_1 wavelength. A discrepancy between the spectra of the R_1 and N_2 centers is the presence of relatively more pronounced R_F and N_2 bands in the R_1 excited-state spectrum; however, as discussed above, this might be due either to systematic errors or to noise problems. The use of more powerful pump laser (e.g., dye laser) for this experiment might give more conclusive results. In any case, the basic features of the R_1 excited-state spectrum correlate very well with the corresponding N_2 data, and further support the proposed F_3 model for the N_2 center.

We also searched for excited states at wavelengths longer than the N_2 absorption band, up to 1.8 μm. Apart from testing theoretical N_2 center models, this knowledge would be useful in explaining the necessity for pulsed operation of the N_2 laser system.[16] Although in principle our apparatus was capable of detecting such transitions, the associated signals would be completely masked by the strong fluorescence of the N_2 center at these wavelengths. We therefore had to resort to a cw-excitation experiment, despite the shortcomings mentioned previously. This experimental setup is essentially similar to the one used in Ref. 26. The cw fluorescence signal was rejected by chop-

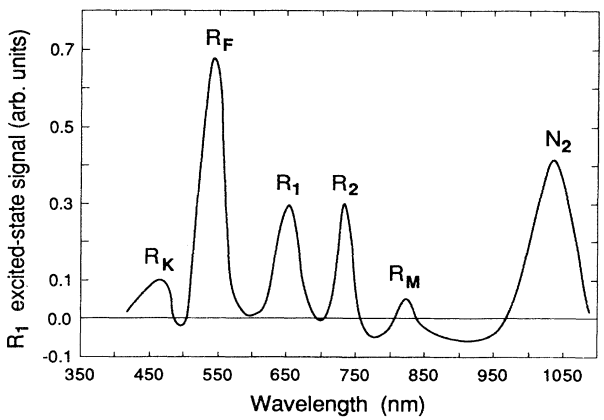

FIG. 9. Excited-state signal of R_1 centers in KCl, pumped with a 633-nm He-Ne laser.

ping only the probe light (before it reached the sample), and using a lock-in amplifier for transmission measurements. Except for the expected partial N_2-band depletion and for heating effects like band broadening, we observed no changes in the absorption spectrum of the crystal between 1 and 1.8 μm. This was true for all pump intensity levels that were tried. This result indicates that there is no N_2 center excited-state absorption overlapping the region of the center fluorescence. This result, in agreement with the trigonal F_3 model energy-level configuration, eliminates one of the possible reasons for the necessity of pulsed laser operation.[16]

VI. EMISSION-POLARIZATION DICHROISM

The polarized absorption and emission properties of a color-center population depend on the direction of the transition dipole moments relative to the center axis, the distribution of the center population among the possible crystallographic directions, and the polarization of the probe light. In order that the dichroic properties are manifested in polarized absorption experiments, the uniform distribution of the color-center population among the possible directions must be altered, by preferential alignment of the centers along a single orientation.[6] However, in fluorescence experiments the use of polarized excitation can produce polarized emission even in the case of random orientation distributions.[36] With judicious choice of pump polarization, the obtained emission intensity pattern as a function of polar angle can reveal the symmetry of the transition moment involved.[6,11,36] In the following, unless otherwise noted, we will assume that the absorption and emission dipole-moment directions coincide. We also assume that the symmetry axes of individual centers are randomly distributed among the allowed crystal directions; i.e., no preferential alignment has occurred.

In our experimental setup, shown schematically in Fig. 10, we used a linearly polarized laser beam incident along the [001] direction of the crystal for the center excitation. The polarization of the pump beam could be set along any direction on the (001) plane; however, in our case, only two pump-beam polarization directions were necessary ([100] and [110]) to reveal the nature of the excited transition dipole moments. The fluorescence emitted along the [001] direction, after passing through a long-pass filter that rejected most of the pump beam, was analyzed with a linear polarizer having its axis on the (001) plane. The transmitted fluorescence was further filtered through a monochromator set at the 1.25-μm peak wavelength of the emission band. A Ge photodiode was used for fluorescence signal detection. For the N_2-band excitation we used a 1.06-μm Nd:YAG laser beam, while for the R_1-band excitation a 633-nm He-Ne laser was used. The recovered fluorescence signal was subsequently normalized with the calibrated polarization response of the apparatus to radiation of the same wavelength. Such calibration was performed by sending unpolarized light through the same optical path, and recording the transmitted intensity for various settings of the analyzer angle.

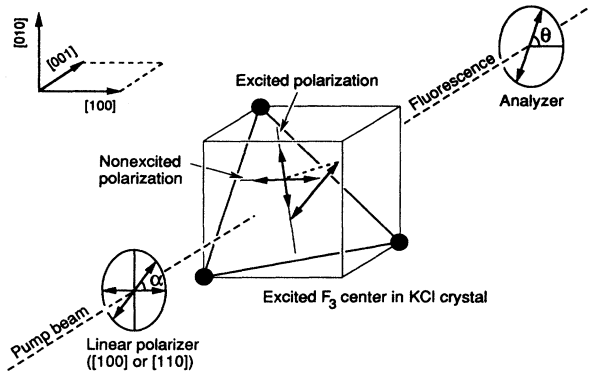

FIG. 10. Schematic arrangement for the polarized emission experiments and analysis scheme for the calculation of the polarized emission intensity patterns (polar graphs of Fig. 11 and 12). In the case of two degenerate transition moments lying on the {111} plane of the trigonal F_3 center, the projection of the pump polarization on the triangle defines the excited dipole moment. The emitted photon can be polarized either along the excited dipole moment (no memory loss), or randomly along any axis lying on the {111} plane (100% memory loss).

The polarized fluorescence intensity values (I), measured in the manner shown in Fig. 10, plotted in polar coordinates as a function of the *analyzer angle* θ with the [100] axis, and compared with the corresponding theoretical predictions, allow determination of the general direction of the transition dipole moment of interest. For example, such plots allow distinction among the cases of simple dipole moments oriented along ⟨100⟩, ⟨110⟩, or ⟨111⟩ directions, or degenerate dipole moments lying on {111} planes[21] (the patterns for nondegenerate ⟨110⟩- and ⟨112⟩-type dipole moments are identical). This method of analyzing the polarized fluorescence is slightly different from that employed in Refs. 11 and 36, where the emission intensity and degree of polarization (defined below) are plotted as functions of the *pump-polarization angle* α with the [100] axis.

The method of calculating the theoretical polarized emission intensity patterns for the cases of ⟨100⟩, ⟨110⟩, or ⟨111⟩ nondegenerate dipole moments is straightforward and need not be discussed here. The calculated patterns are described in Ref. 21. For the case of degenerate dipole moments lying on {111} planes—as is the case of $E \rightarrow E$ transitions of the trigonal F_3 center—the analysis scheme for the intensity-pattern calculation is shown in Fig. 10. The pump-photon polarization vector determines a set of two orthogonal axes on the plane of each F_3 triangle. For each F_3 center only one of these dipole-moment axes is excited during the absorption process. Assuming that no polarization memory loss occurs following absorption, the polarization of the emitted photon will lie exactly along the excited direction. In this case, the emission intensity pattern will be determined by the angles between the excited directions and the analyzer axis, once all possible F_3 orientations and excitation strengths are taken into account. The intensity-

pattern functional forms will be $I \propto 1+\sin 2\theta$, and $I \propto 1+3\cos^2\theta$, for [110] and [100] pump polarizations, respectively. However, if polarization-memory loss occurs (experimental justification of this assumption as well as theoretical mechanisms for such memory loss will be presented later), then the emitted photon can have any polarization on the $\{111\}$, F_3 plane. In this case the emission intensity pattern will be determined by the angles between the F_3 planes and the analyzer axis (with plane excitation strengths taken into account). The intensity-pattern functional forms will be $I \propto 1+\frac{1}{4}\sin 2\theta$, and $I=$const, for [110] and [100] pump polarizations, respectively.

The polarized fluorescence patterns obtained from the N_2 centers are shown in Fig. 11 for two cases of pump polarization. The degree of emission polarization p [defined as $p=(I_{\parallel}-I_{\perp})/(I_{\parallel}+I_{\perp})$, where $I_{\parallel}$ and $I_{\perp}$ are the emission intensities with polarization parallel or perpendicular to the pump-light vector] is approximately 28% for [110] excitation and approximately 7% for [100] excitation. For comparison, the polarized emission experiments were repeated using a He-Ne laser beam to pump the R_1 absorption band, with the fluorescence again monitored at 1.25 μm. The fluorescence intensity patterns obtained are shown in Fig. 12, and the observed degree of polarization p is approximately 68% for [110] excitation and 65% for [100] excitation.

In spite of the differences between Figs. 11 and 12, the experimental results for both the R_1- and N_2-emission cases can be interpreted and accurately calculated in a way consistent with the trigonal F_3-model framework. This interpretation is based on the fluorescence patterns of degenerate orthogonal dipole moments (corresponding to degenerate energy transitions) lying on the $\{111\}$ planes of the F_3 triangles. According to the trigonal F_3 model, both the R_1 and N_2 bands originate from $\{E \rightarrow E\}$ transitions of the same center (Fig. 8), which occur between ground and excited doubly degenerate vibronic levels.[7] An $E \rightarrow E$ transition is characterized by a combination of orthogonal dipole moments lying on the $\{111\}$ plane of the defect. One such combination is a pair of orthogonal $\langle 110 \rangle$ and $\langle 112 \rangle$ moments, although the choice of axes on each $\{111\}$ plane can be completely arbitrary. In the case of the N_2 emission (Fig. 11) the additional assumption of total emission-polarization

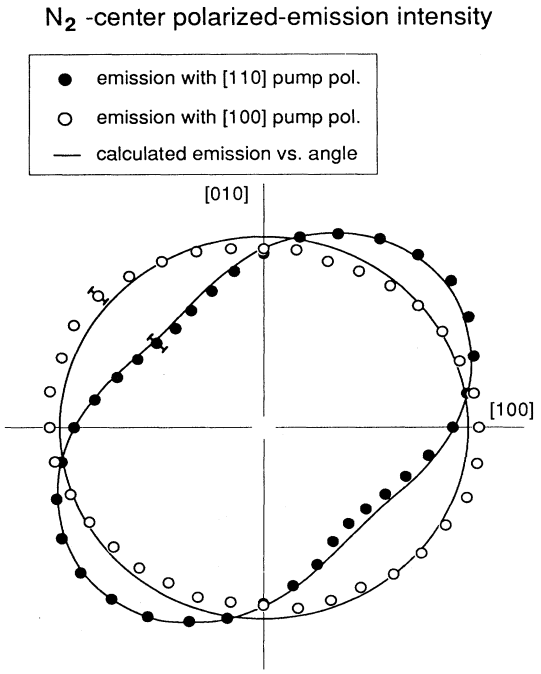

FIG. 11. Polarized-emission intensity (in polar coordinates) from randomly oriented N_2 centers in KCl as a function of the analyzer angle, for two cases of pump polarization (pump: 1.06-μm Nd:YAG laser). Solid circles: measured intensity I for [110]-polarized pump. Open circles: measured intensity for [100]-polarized pump. Continuous curves: calculated (theoretical) patterns, having the functional forms $I \propto 1+\frac{1}{4}\sin 2\theta$ and $I=$const for [110] and [100] pump polarizations, respectively. These patterns were calculated for degenerate orthogonal dipole moments lying on $\{111\}$ planes, with the assumption that the polarization memory is completely lost in the absorption-emission cycle. Experimental arrangement and theoretical analysis scheme is shown in Fig. 10 and explained in the text.

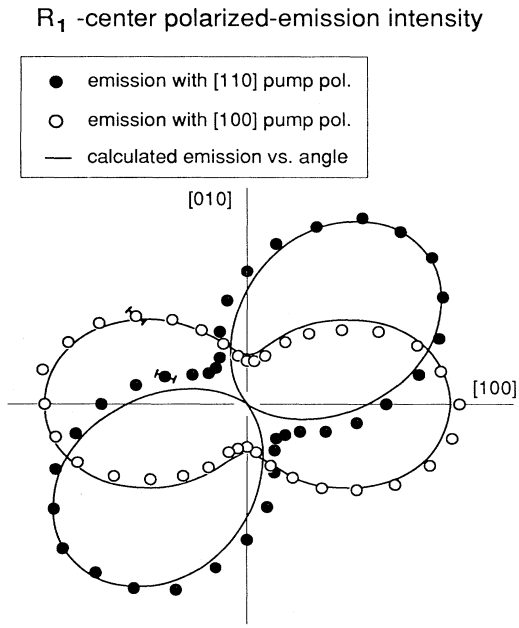

FIG. 12. Polarized-emission intensity (in polar coordinates) from R_1 centers in KCl as a function of the analyzer angle, for two cases of pump polarization (pump: 633-nm He-Ne-laser). Solid circles: measured intensity I for [110]-polarized pump. Open circles: measured intensity for [100]-polarized pump. Continuous curves: calculated (theoretical) patterns, having the functional forms $I \propto 1+\sin 2\theta$ and $I \propto 1+3\cos^2\theta$ for [110] and [100] pump polarizations, respectively. These patterns were calculated for degenerate orthogonal dipole moments lying on $\{111\}$ planes, with the assumption that the polarization memory is totally preserved in the absorption-emission cycle. Experimental arrangement and theoretical analysis scheme are shown in Fig. 10 and explained in the text.

"memory loss" is required, in order to theoretically calculate the N_2 polarized emission patterns that match the experimental points. However, in the case of the R_1 emission (Fig. 12), the accurate calculation of the experimentally observed pattern requires the assumption of only some minor emission-polarization memory loss[21] (assumed to be zero in Fig. 12 calculations for the sake of simplicity). It is not clear at the moment how the polarization memory is preserved in the R_1 absorption-emission cycle, while it is totally lost in the N_2 cycle, since, according to the F_3-model interpretation, a large (≈ 0.67 eV) radiationless relaxation from the R_1 to the N_2 energy level precedes the emission. A possible reason for the R_1 versus N_2 emission polarization disagreement might be related to the fact that we used monochromatic laser light to pump the respective absorption bands, thus exciting transitions between specific vibronic levels with particular polarization selection rules. Repeating these experiments at different pump wavelengths, as well as measuring the emission-polarization properties of the other F_3-center bands (R_2 and R_M), may resolve the observed discrepancy.

Now we come to the question of possible mechanisms that can account for polarization-memory loss between the N_2 absorption and emission. This phenomenon can be attributed to either random perturbations (like strain or electric fields) which may cause splitting and mixing of the doubly degenerate E vibronic levels, or to depolarization of the emission during radiationless decay to the lowest vibrational level in the electronic excited state. In the first interpretation, each F_3 plane should have a different *fixed* set of orthogonal-transition dipole-moment axes (corresponding to the split energy levels), their direction now determined from the particular perturbation symmetry. A Rabi oscillation between the two originally degenerate excited levels can result in the emission of a photon polarized along any direction on the {111} defect plane, if the precession period is on the order of the radiative lifetime or shorter. It can be easily seen that, for an N_2-emission lifetime of ≈ 200 nsec, energy-level splittings as small as 10^{-8} eV are adequate to produce such short precession periods. Then, on the average, the fluorescence emitted from a statistical ensemble of similarly oriented trigonal F_3 centers should be totally unpolarized on the triangle plane. In the second interpretation, the photon polarization is completely randomized during the process of relaxation to the lowest vibrational level of the excited electronic state, prior to the emission. In both interpretations, the observed remaining emission polarization (see Fig. 11) is due to purely geometrical reasons, i.e., due to the F_3 triangle orientation relative to the exciting polarization (different F_3 orientations absorb with different strengths, and this anisotropy is partially relayed to the emission, despite the depolarization effects).

Comparing our polarized emission results with previous published work, we noted disagreement in many cases. Our data on the R_1 fluorescence shows a highly polarized emission from the excitation of this band, in disagreement with some older studies[11,26,28] which find degrees of polarization p no higher than 20–25 %. However, we noticed inconsistencies in several of those cases; for example, Van Doorn[11] also reported an unacceptably low p for the F_2 band, a fact which probably indicates a systematic error with his measurements of p, while Compton and Klick[26] noticed strong sample-dependence of their p values. Also, we should mention that our general analysis disagrees with a statement (but not with the results) of Ref. 8, which claims that it is difficult to distinguish between a ⟨111⟩ moment and a degenerate ⟨112⟩ moment (such as that of the R center) in dichroic emission. Finally, our conclusions disagree with those of Ref. 27, where a ⟨111⟩-type dipole moment is determined for the R_1, R_2, and N_2 transitions. We reject this possibility for both the R_1 and the N_2 transitions on the basis of the observed polarized emission patterns (Figs. 11 and 12), which exhibit nonzero degrees of polarization in the case of [110] excitation.[21] It is worth noting that the reliability and accuracy of our experimental method was checked by applying it to the case of the F_2^+:O^{2-} center in NaCl,[21] a defect known to have a ⟨110⟩ fundamental transition dipole moment.[17] In that case, the fit of the experimental points to the theoretically expected pattern was excellent, and the observed degrees of polarization p matched those calculated by 1%.

In conclusion, the agreement between observed and calculated intensity patterns (Figs. 11 and 12) is very good, and strongly supports the trigonal F_3-center model for both the N_2 and R_1 bands. A puzzling phenomenon is the retention of polarization memory in the R_1 excitation in contrast to the loss of memory in the N_2 excitation of lower energy. This unresolved question is worth further investigation both experimentally and theoretically.

VII. *N*- AND *R*-CENTER REORIENTATION PROPERTIES

The reorientation of a color center consists of flipping the defect's axis between two of the various possible crystallographic directions. Color-center reorientation may occur through thermal or optical excitation.[6,17] In the case of polarized optical excitation, preferential alignment of the color-center population along a particular crystallographic direction is possible. Such aligned populations exhibit dichroic absorption and emission properties in experiments using polarized probe light.

In previous studies, qualitatively similar R_1, R_2, and N_2-band dichroism has been reported to develop under prolonged illumination with polarized R_1-band light at temperatures close to 300 K.[7,27,37] In an attempt to verify these findings, we illuminated crystals for several hours with either 633-nm He-Ne laser or broadband red (640–680 nm) light, incident along the [001] direction and polarized along [110], at temperatures ranging from 77 to 300 K. Alignment of the dipole moments was probed using polarized absorption and emission techniques, with probe light of the appropriate wavelength incident along [001] and polarized along [110] or [−110]. The probe-light intensity in our experiments was much weaker than the intensity of the aligning illumination, to

prevent possible center reorientation effects in the course of the measurements. For the same reason, probing of the alignment was performed at 77 K, where reorientation effects were not observable.

Center alignment was indicated by differences in either the absorbances or the fluorescence signals corresponding to the two probe-light polarizations. Dichroic effects were observed only when the alignment process was performed at temperatures above 240 K. However, at these elevated temperatures significant aggregation effects were concurrently taking place under the action of red light during the required long illumination periods; therefore, in the case of the N_2 band, it was difficult to distinguish between signal changes due to potential center alignment or changes due to aggregation. As a result, we never observed pure orientational bleaching, even for crystals where the aggregation process had reached the approximate steady-state (plateau) region of Fig. 3.

When the color-center alignment process was performed using [110]-polarized R_1-band illumination, some enhancement of the $[-110]$-polarized N_1- and N_2-band absorbances relative to the [110]-polarized absorbances was observed. Similar dichroic changes were observed in the R_1 and R_2 bands, while the F_2 band remained unaffected. Typical absorption-coefficient ratios α_p/α_t for probe-light polarizations parallel and transverse to the aligning light polarization, respectively, were

$$\alpha_p/\alpha_t = 0.87\pm0.01(R_1)\ ,\quad 0.88\pm0.01(R_2)\ ,$$
$$0.90\pm0.03(N_1)\ ,\quad 0.87\pm0.03(N_2)$$

at the corresponding band peaks.

The observed orientational population differences cannot be due to anisotropic photoaggregation, since then it follows that the trigonal F_3 centers form preferentially on those $\{111\}$ planes least excited by the $\langle 110\rangle$ aggregating light polarizations; such an effect would be hard to interpret. On the other hand, if the population differences are due to reorientation, then the observed results can be expected in analogy with the general optical reorientation behavior of color centers,[6,17] i.e., alignment of the transition dipoles along those crystal directions which least absorb the exciting light. Specifically, these results are consistent with the model of trigonal F_3 centers (having their N- and R-transition dipole moments on $\{111\}$ planes), preferentially populating the (111) and $(11\bar{1})$ planes relative to the $(\bar{1}11)$ and $(1\bar{1}1)$ planes under the action of [110]-polarized R_1-band illumination.

A calculation based on the hypothesis that dipole-population reorientation rates are proportional to the excitation strength of each dipole direction leads to the result that upon equilibrium each direction is populated inversely proportional to $\cos^2\phi$, where ϕ is the angle between the dipole moment and the exciting polarization. This hypothesis, applied to the case of F_3 triangles which have orthogonal degenerate dipole moments lying on their $\{111\}$ planes, predicts that the total center population, N_0, is distributed as $\frac{3}{8}N_0$, $\frac{3}{8}N_0$, $\frac{1}{8}N_0$, $\frac{1}{8}N_0$, on the (111), $(11\bar{1})$, $(1\bar{1}1)$, and $(\bar{1}11)$ planes, respectively, in the case of [110]-polarized aligning radiation (these populations are inversely proportional to $\cos^2(90°-\omega)$, where ω is the angle between the [110] exciting polarization and the vector $\hat{1}$ perpendicular to each triangle). Such an aligned population distribution presents different absorption coefficients α_p, α_t, to [110] and $[1\bar{1}0]$ probe-light polarizations, respectively, having a contrast ratio of $\alpha_p/\alpha_t=\frac{3}{5}$. Since a low value of α_p/α_t corresponds to a high degree of alignment, the theoretical F_3-center orientation dichroism is small compared to that of other simpler color-center dipoles.[17]

The experimentally observed weak F_3-center reorientation dichroism is consistent with these model predictions, in the sense that the experiment produces contrast values α_p/α_t consistent with the theoretical limit of $\frac{3}{5}$. This is additional indication for the validity of the trigonal F_3 model.

VIII. DISCUSSION

Most of the experimental data presented in this paper supports the interpretation of the laser-active N_2 transition in KCl as a transition of the trigonal F_3 center. Although Pick's tetrahedral F_4 model[4,6] has not been directly disproven, we found no experimental evidence supporting his proposal. Furthermore, Stoneham's calculations[38] also conclude that the Pick model is not responsible for the N_2 transition, since transitions of suitable energy from the ground state would be forbidden by the spin selection rule.

In view of the experimental results presented in this and previous work, the relation between the N_1 and N_2 bands remains an open question. The theoretical calculations are still too crude to reliably estimate the magnitude of the N-transition energy splitting. We will briefly discuss here the available experimental evidence.

Previous arguments in support of the identical nature of the N_1 and N_2 bands have been based mostly on the coincidence of the emission bands obtained from these two centers in KCl.[7,8,13] However, we believe that this argument is not compelling, since in our studies of N and R centers in NaCl we have also obtained practically identical fluorescence bands from apparently dissimilar centers.[39] The fact that their fluorescence properties are so similar presents interesting questions about the transitions of multielectron color centers.

Arguments based on the similar growth rates and almost constant band ratios for the N_1 and N_2 bands (Figs. 3–5) are not conclusive either. These arguments simply imply that both centers consist of the same number of F centers; their electronic and/or spatial structure can be quite different.[8] Furthermore, parallel experiments in NaCl measured quite different growth rates for the N_1 and N_2 bands in that host lattice, depending on the photoaggregation process.[39] The conclusion of our NaCl N- and R-center studies was that the N_1 and N_2 centers are of different nature. This conclusion is consistent with previous piezospectroscopic studies of the N_1 center in NaCl indicating that this defect has a planar F_4 structure.[9]

Among the indications supporting the theory of com-

mon origin of the N_1 and N_2 bands, the hardest to refute are probably the equal polarizability of the two bands (see data presented in Sec. VII), and the similar stress-induced dichroism.[7] Although none of these can be considered decisive, they lend considerable support to the single-N-center model.

The measurement of the F_3-center excited-state spectrum, however, which we consider the most sensitive tool for electronic structure characterization provides strong evidence that the N_1 and N_2 bands are due to different centers. This technique, which probes several transitions of the defect in question, is in principle less sensitive to band overlaps or other wavelength coincidences. Two distinct experiments probing the excited-state transitions of the trigonal F_3 center, one using N_2-band excitation and the other using R_1-band excitation, indicated that the N_1 band is not a transition of this defect. However, the proper interpretation of this data requires us to take into account any possibilities of band cancellations due to perfectly overlapping competing transitions. For example, a transition from the first excited state to some higher level would compete with a transition originating from the ground state, if their peaks, widths, and oscillator strengths were identical (which we consider very unlikely). Another more subtle possibility could involve the creation of short-lived charged centers through ionizing action by the pump photons ($2F_3 \rightarrow F_3^- + F_3^+$). Such dynamically maintained populations would produce absorption-modulation signals having negative sign in the spectra of Figs. 7 and 9. Thus, the signal due to F_3^- centers could nicely account for the broad negative background extending between 700 and 950 nm, since such broad bands are characteristic of "primed" color centers, while the F_3^+ absorption, coincident in wavelength and width with the N_1 band,[8] could subtract from and annihilate the $(F_3)_{N_1}$-transition signal. Though intriguing, such an interpretation still needs to demonstrate an unlikely conspiracy between the F_3^+ and $(F_3)_{N_1}$-band relative oscillator strengths and the ionization probability of the F_3 center under 1.06-μm excitation, in order to produce the desired F_3^+ and $(F_3)_{N_1}$ band mutual cancellation. Additionally, the F_3-center ionization probability, and therefore the efficiency of the electron-transfer process, is expected to vary with pump wavelength, rendering the perfect band cancellation in both Figs. 7 and 9 spectra impossible. While we consider the electron-transfer model rather improbable, such an interpretation of the excited-state data cannot be totally rejected, and further work in KCl and other host lattices is necessary until a firm conclusion on the nature of the N_1 band can be established.

Given the fact that there exists a variety of N centers with overlapping transitions, it is difficult to prove that it is precisely the $(F_3)N$ transition which is responsible for the lasing action in KCl. The fact that the F_3 nature of the N_2 band is most clearly revealed in crystals which have been prepared for optimum laser operation permits us to characterize the lasing defect as a trigonal F_3 color center. A conclusive proof of this assignment would be the achievement of lasing action, with the same tuning curve as the N_2-center laser, by pumping the higher R_1 or R_2 transitions. This experiment would probably require a pulsed pump source with characteristics similar to the Q-switched Nd:YAG laser that has been used to pump the N_2-center system.[16] With the development of several new powerful laser sources this may soon become an easy task to achieve. Analogous experiments on the N_1 band in KCl could also determine conclusively whether this band is a transition of the same defect as the N_2 band or not.

Finally, we will try here to interpret the pulsed operation of the N_2-center laser in view of the results presented in this work. The presently known spectroscopic data (N_2-center density $\approx 1.7\times 10^{16}$ centers/cm^3, emission lifetime $\tau \approx 200$ nsec, emission wavelength $\lambda = 1.25$ μm, emission cross section $\sigma = 4\times 10^{-17}$ cm^2) together with our laser parameters (beam waist $\omega_0 = 30$ μm, effective crystal thickness $1 = 2.4$ mm, output coupling 7%) indicate a threshold inversion density $\Delta N_t \approx 0.75\times 10^{16}$ centers/cm^3, which is comparable to the total available N_2-center density. Given the thermal limit of 0.6 W for the average absorbed pump power and the low (4%) power-conversion efficiency,[16] we calculate that in the best of conditions the color-center laser would barely reach threshold in continuous wave (cw) operation. It is still not clear from these arguments, however, whether the necessity of pulsed N-center laser operation is merely due to high threshold values (which might be overcome with improved laser design and pumping schemes), or whether it is linked to an intrinsic feature of the N_2 center.

In our previous paper[16] we suggested several possible intrinsic reasons for the necessity of pulsed pumping. Among these, the possibility that excited-state transitions overlap the N_2 band and cause excess loss seems to be ruled out by the present data. It is not known whether such transitions are predicted by the F_3 model, since theoretical calculations exist only for transitions originating from the ground state. Another quoted possibility, a low absolute quantum efficiency for the N_2 emission, especially under very intense excitation, is still a reasonable assumption. We have not yet fully investigated this, due to difficulties in reproducing in our spectrometer the conditions occurring in the pumped crystal spot during laser operation. Data obtained under low-intensity excitation (Fig. 6) indicate that the emission quantum efficiency decreases as a function of temperature, even around 77 K. Since the emission intensity does not seem to level off to some constant value as the temperature approaches 77 K, the quantum efficiency must still be smaller than unity at 77 K (although the simple criterion of Dexter, Klick, and Russell on nonradiative processes, as quoted in Ref. 40, predicts high radiative efficiency for the N_2-center absorption-emission cycle). In any case, the almost certain existence of several color-center absorptions overlapping the N_2 band could lead to wrong conclusions regarding the true efficiency of the N_2 absorption-emission cycle.

The third possibility that we previously mentioned,[16] namely the creation of an excited-state bottleneck due to transitions between spin multiplet states, may fit nicely in the F_3 model of the N_2 center. As shown in Fig. 8, the

spin-quartet A_1 state lies 0.94 eV lower than the N_2 doublet E state of the trigonal F_3 center. Electric dipole transitions between doublet and quartet states are theoretically forbidden in the continuum model of the center; however, in the crystal environment such transitions may be weakly allowed, and in the case of the F_3 center in KCl they have been experimentally observed.[31] As might be expected, the associated lifetimes are very long (15 sec for the quartet emission as determined by the associated fluorescence at ≈ 4.4 μm).[31] If some fraction of the excited N_2 centers "leaks" to the quartet level instead of radiatively returning to the ground state, a bottleneck in fast pump cycle is created, due to the extremely long lifetime of the quartet relaxation. A simple calculation based on rate equations indicates that a branching ratio b from the N_2 doublet to the A_1 quartet level as low as 10^{-8} is already sufficient to quench the cw laser operation. Although such a small b would imply that cw lasing could take place for several seconds before the quartet level is sufficiently populated for the lasing process to quench, the lack of any experimental evidence of such short-term cw operation can be explained by other laser factors. Of course, less severe values of b are quite possible, and it is worth examining the compatibility of b with the range of duty-cycles for which steady-state pulsed laser operation has been experimentally achieved.[16] For example, for operation with 10-μsec pump-pulse duration at a repetition rate of 10 KHz, a $b \leq 2 \times 10^{-7}$ is required, implying a reasonable lifetime of $\tau \geq 1.1$ sec for the "leak" from the doublet to the quartet level. Therefore, the trigonal F_3 model can also account for the necessity of pulsed operation of the N_2 laser system.

In conclusion, we have studied the formation and optical properties of the N_2 laser-active color center in KCl that are relevant to laser operation. All experimental data presented in this work can be interpreted in the context of the trigonal F_3 model. Although alternative models cannot yet be unambiguously refuted, it appears that the agreement between experimental results and available theoretical predictions is satisfactory for the proposed configuration. Further study of the defect in other host lattices is needed to confirm the proposed model and assist in the discovery of other similar, tunable, laser-active systems.

ACKNOWLEDGMENTS

The authors would like to thank Professor R. H. Silsbee for many helpful discussions and insightful suggestions on the interpretation of experimental data. This research was funded by the Materials Science Center of Cornell University.

[1] J. P. Molnar, Ph.D. thesis, MIT (1940).
[2] E. Burstein and J. J. Oberly, Phys. Rev. **76**, 1254 (1949).
[3] S. Petroff, Z. Phys. **127**, 443 (1950).
[4] H. Pick, Z. Phys. **159**, 69 (1960).
[5] S. Schnatterly and W. D. Compton, Phys. Rev. **135**, A227 (1964).
[6] W. D. Compton and H. Rabin, in *Solid State Physics,* edited by F. Seitz and D. Turnbull (Academic, New York, 1964), Vol. 16.
[7] R. H. Silsbee, Phys. Rev. **138**, A180 (1965).
[8] I. Schneider and M. N. Kabler, J. Phys. Chem. Solids **27**, 805 (1966).
[9] A. E. Hughes, Proc. Phys. Soc. **87**, 535 (1966).
[10] I. Schneider, J. Appl. Phys. **59**, 1086 (1986).
[11] C. Z. van Doorn, Philips Res. Repts. Suppl. 4 (1962).
[12] I. Schneider and H. Rabin, Phys. Rev. **140**, A1983 (1965).
[13] I. Schneider, Solid State Commun. **4**, 91 (1966).
[14] J. Rolfe and S. R. Morisson, Phys. Rev. B **15**, 3211 (1977).
[15] D. B. Fitchen, R. H. Silsbee, T. A. Fulton, and E. L. Wolf, Phys. Rev. Lett. **11**, 275 (1963).
[16] E. Georgiou, T. J. Carrig, and C. R. Pollock, Opt. Lett. **13**, 978 (1988).
[17] E. Georgiou, J. F. Pinto, and C. R. Pollock, Phys. Rev. B **35**, 7636 (1987).
[18] A. Chandra and D. F. Holcomb, J. Chem. Phys. **51**, 1509 (1969).
[19] E. Sonder, Phys. Rev. B **2**, 4189 (1970).
[20] S. Hattori, J. Phys. Soc. Jpn. **17**, 1454 (1962).
[21] E. Georgiou, Ph.D. thesis, Cornell University (1989).
[22] Filtering in the 750–1000-nm region was accomplished with a combination of sharp longpass (Schott OG-750) and shortpass (Corion LS1000) filters, respectively.
[23] K. Asai and A. Okuda, J. Phys. Soc. Jpn. **21**, 2197 (1966).
[24] St. Petroff, M. Mladenova, and M. Georgiev, Solid State Commun. **9**, 2095 (1971).
[25] W. E. Bron, Phys. Rev. **125**, 509 (1962).
[26] W. D. Compton and C. C. Klick, Phys. Rev. **112**, 1620 (1958).
[27] F. Okamoto, Phys. Rev. **124**, 1090 (1961).
[28] J. Lambe and W. D. Compton, Phys. Rev. **106**, 684 (1957).
[29] G. Chiarotti and U. M. Grassano, Nuovo Cimento **46B**, 78 (1966).
[30] H. Seidel, M. Schwoerer, and D. Schmid, Z. Phys. **182**, 398 (1965).
[31] J. M. Ortega, Solid State Commun. **25**, 885 (1978).
[32] A. M. Stoneham, *Theory of Defects in Solids* (Clarendon, Oxford, 1975), pp. 631–652.
[33] S. Wang and C. Chu, Phys. Rev. **147**, 527 (1966).
[34] A. Maisonneuve and J. Margerie, J. Phys. C **12**, 1937 (1979).
[35] R. C. Kern, G. G. DeLeo, and R. H. Bartram, Phys. Rev. B **24**, 2211 (1980).
[36] P. P. Feofilov, *The Physical Basis of Polarized Emission,* Russian transl. (Consultants Bureau, New York, 1961).
[37] M. Hirai, M. Ikezawa, and M. Ueta, J. Phys. Soc. Jpn. **17**, 1483 (1962).
[38] A. M. Stoneham, Proc. Phys. Soc. **88**, 135 (1966).
[39] E. Georgiou and C. R. Pollock, Phys Rev. B **40**, 6321 (1989).
[40] R. H. Bartram and A. M. Stoneham, Solid State Commun. **17**, 1593 (1975).